Journal of Alloys and Compounds 509 (2011) 8779–8782

Contents lists available at ScienceDirect

Journal of Alloys and Compounds

journal homepage: www.elsevier.com/locate/jallcom

Effects of raw materials on microstructure and dielectric properties of $PbZrO_3$ antiferroelectric thin films prepared via sol–gel process

Yunying Liu[a], Xihong Hao[b,*], Jing Zhou[c], Jinbao Xu[d], Shengli An[b]

[a] School of Chemistry and Chemical Engineering, Inner Mongolia University of Science and Technology, Baotou 014010, China
[b] School of Materials and Metallurgy, Inner Mongolia University of Science and Technology, Baotou 014010, China
[c] State Key Laboratory of Advanced Technology for Materials Synthesis and Processing, Wuhan University of Technology, Wuhan 430070, China
[d] Xinjiang Key Laboratory of Electronic Information Materials and Devices, Xinjiang Technical Institute of Physics and Chemistry, Chinese Academy of Sciences, Urumqi 830011, China

ARTICLE INFO

Article history:
Received 10 February 2011
Received in revised form 15 June 2011
Accepted 16 June 2011
Available online 22 June 2011

Keywords:
Electronic materials
Chemical synthesis
Microstructure
Dielectric response

ABSTRACT

In this work, we report on two kinds of $PbZrO_3$ (PZO) antiferroelectric (AFE) thin films with a thickness of about 700 nm, which were fabricated by using zirconium isopropoxide and zirconium nitrate as starting materials, respectively. The effects of the raw materials on microstructure and electrical properties of the PZO AFE films were studied in detail. X-ray diffraction and scanning electron microcopy results showed that the PZO films obtained from zirconium isopropoxide were highly (1 1 1)-oriented and had a more uniform surface microstructure. As a result, the PZO films from zirconium isopropoxide accordingly displayed better electrical properties, such as lager dielectric constant, increased saturated polarization, and smaller leakage current.

© 2011 Elsevier B.V. All rights reserved.

1. Introduction

$PbZrO_3$ (PZO) was the first found antiferroelectrics (AFEs), in which lead ions had an anti-parallel shift along the ⟨1 1 0⟩ direction [1]. So there are no net polarization existed along a–b plane in PZO. However, by applying sufficiently high dc electric field, the anti-parallel arranged dipoles could be induced into same direction, which is corresponded the phase transition from AFE to ferroelectric (FE) [2]. During the electric field-induced phase switching procedure between AFE and ferroelectric, AFEs usually display larger field-induced strains, higher energy storage density, considerable pyroelectric coefficient, and giant electrocaloric effect, which make them potential for applications in micro-actuators, infrared-detectors, digital memories, high energy storage capacitors and cooling devices [3–5]. Therefore, lead-based AFE materials in bulk ceramic and film forms are attracting increasing attention [6–11]. However, in contrast to PZO films, the room temperature field-induced AFE–FE switching in PZO bulk ceramic has not been realized because of its lower breakdown field. At the same time, AFE films have lower operating voltage and are easily integrated with silicon. Thus, AFEs in film form are more likely to be used in practice.

Up to now, in order to optimize their final properties, a number of papers have been reported on AFE thin and thick films [12–15]. Generally speaking, these studies were mainly focused on two aspects. One was the growth and orientation control of AFE films. Another was the study on phase switching process as a function of dc field and temperature. To the best of our knowledge, effects of raw materials on the final electrical properties of AFE thin films have been rarely reported. Thus, in this work, two kinds of PZO thin films were fabricated by using zirconium isopropoxide and zirconium nitrate as Zr resource, respectively. The aim is to investigate microstructure and electrical properties of the PZO films prepared from the different raw materials.

2. Experimental details

The $PbZrO_3$ (PZO) thin films in both cases were fabricated by using a sol–gel route. Fig. 1(a) gives the flow diagram of the solution preparation from zirconium isopropoxide. In this case, lead acetate trihydrate (99.5%, Sinopharm Chemical Reagent Co., Ltd., China) and zirconium isopropoxide (70% in propanol, Aldrich) were selected as the raw materials, and glacial acetic and deionized water were used as a solvent. Firstly, lead acetate trihydrate with 10% excess and acetic acid were mixed and distilled at 110 °C for 1 h. The excessive lead was used to compensate lead loss during annealing and prevent the formation of pyrochlore phase. Secondly, after the mixed solution was cooled to room temperature, zirconium propoxide were added and stirred for 30 min. At the same time, distilled water was added in 20 times to stabilize the solution during the mixing process. Finally, the solution was adjusted to 0.3 M using acetic acid and 2-ethoxyethanol, which was labeled as PZO-1. The addition of 2-ethoxyethanol lowered the surface tension of the solution to improve the wettability. Fig. 1(b) shows the flow diagram of the solution preparation from zirconium nitrate. In this case, lead acetate trihydrate and zirconium nitrate were used as

* Corresponding author. Tel.: +86 472 5951572; fax: +86 472 5952571.
E-mail address: xhhao@imust.cn (X. Hao).

0925-8388/$ – see front matter © 2011 Elsevier B.V. All rights reserved.
doi:10.1016/j.jallcom.2011.06.067

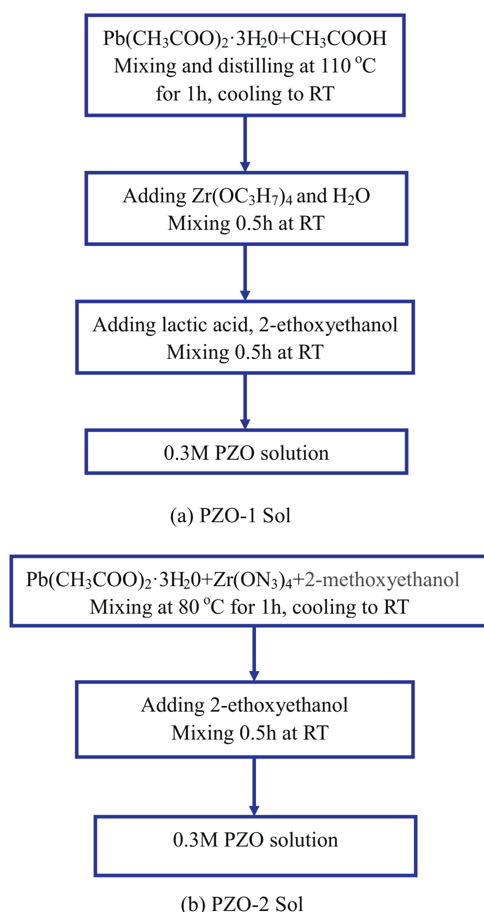

Fig. 1. Flow diagram of solution synthesis processing for the PZO AFE films from different starting materials.

the starting materials. 2-methoxyethanol was solvent. Lead acetate trihydrate with 10% excess and zirconium nitrate (99%, Sinopharm Chemical Reagent Co., Ltd., China) were mixed in 2-methoxyethanol at 80 °C for 1 h. When the solution was cooled to room temperature, it was also adjusted to be 0.3 M using 2-methoxyethanol. This solution was labeled as PZO-2.

After aging for 24 h, the two solutions were used to deposit films on Pt(1 1 1)/Ti/SiO_2/Si(1 0 0) substrates by the spin-coating method. Thicknesses of Pt, Ti and SiO_2 of the substrate were 150, 20 and 300 nm, respectively. Each PZO layer was spin-coated at 3000 rpm for 20 s and pyrolyzed at 450 °C for 10 min. The spin-coating and heat-treatment were repeated several times to obtain desired thickness. A capping layer from 0.4 M PbO precursor solution, which was prepared from lead acetate trihydrate, was deposited before these films went through a final anneal at 700 °C for 30 min to form perovskite phase. This capping layer served to prevent excessive lead loss and ensure the formation of single perovskite phase of PZO. Final thickness of the PZO films was 700 nm for both cases. For convenience, the PZO films prepared from zirconium isopropoxide also were labeled as PZO-1, and the films from zirconium nitrate were labeled as PZO-2.

Phase structure and microstructure of the films were investigated by using X-ray diffractometer (XRD BRUKER D8 Advance diffractometer) and scanning electron microscopy (SEM JSM EMP-800, JEOL, Tokyo, Japan). Thicknesses of the films were measured by F20 system (Filmetrics). For electrical measurements, sandwich figuration capacitors were fabricated by dc sputtering gold top electrodes of 0.5 mm diameter onto the PZO AFE thin films through a shadow mask. Post-annealing for the top electrodes at 200 °C for 20 min was performed to improve the adhesion of gold. Field-induced polarization hysteresis (P–E) loops at 1 kHz and dc current-field curves of the PZO thin films were measured by a Radiant Technology ferroelectric tester. Frequency, temperature and field-dependent dielectric properties of the films were analyzed by using a TH2828 LCR meter.

3. Results and discussion

Fig. 2 shows XRD patterns of the PZO films prepared from different Zr resources. The lattice indices of the peaks were labeled according to pseudocubic structure. Clearly, after annealed at

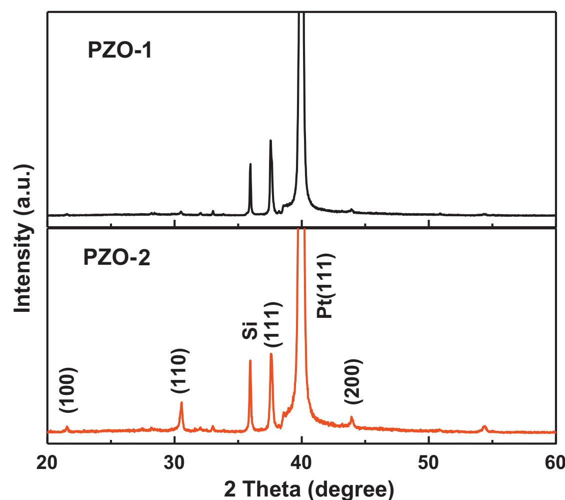

Fig. 2. XRD patterns of the PZO AFE films from different starting materials.

700 °C for 30 min, the two PZO films had crystallized into a pure perovskite phase. However, it is found that the PZO films from zirconium isopropoxide have a highly (1 1 1)-preferred orientation while the films from zirconium nitrate display a random orientation. This means that the growth orientation of PZO AFE films is strongly dependent on their starting materials.

SEM images of the PZO films are shown in Fig. 3. Evidently, PZO-1 sample has a more uniform and crack-free characteristic, as compared with PZO-2 sample. However, necks between grains are formed in both cases. Similar microstructures were also observed

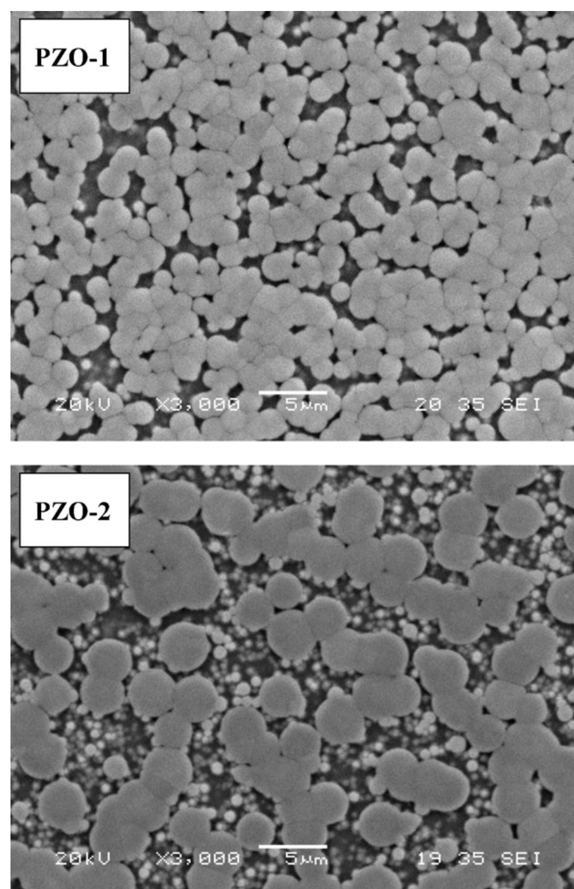

Fig. 3. SME images of the PZO AFE films from different starting materials.

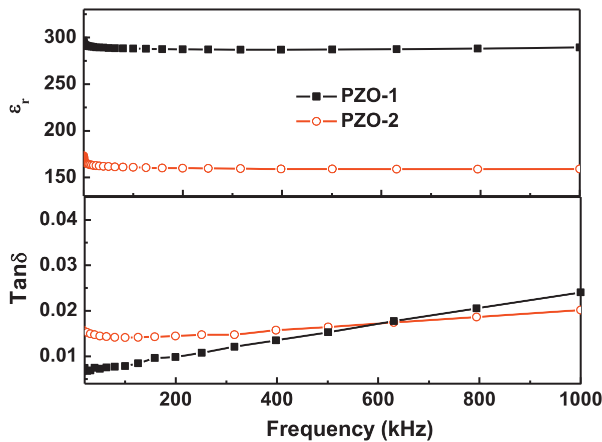

Fig. 4. Frequency-dependent dielectric constant and dielectric loss of the PZO AFE films from different starting materials.

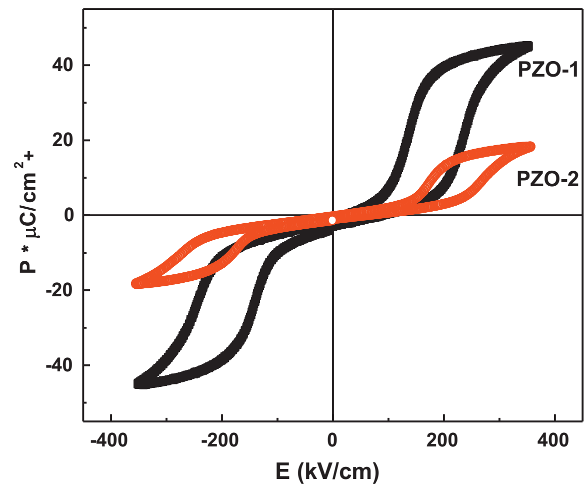

Fig. 5. P–E loops of the PZO AFE films from different starting materials.

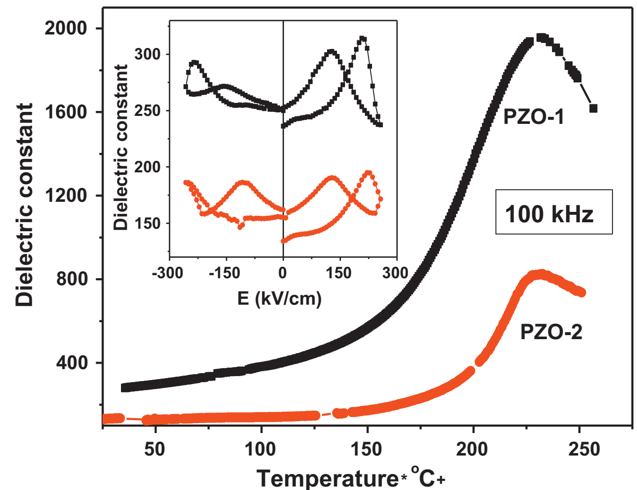

Fig. 6. Temperature-dependent dielectric constant of the PZO AFE films from different starting materials. The inset shows dielectric constant with respect to dc electric field of the PZO AFE films from different starting materials.

in $Pb(Zr,Ti)O_3$ and $Ba(Zr,Ti)O_3$ thin films [16,17]. According to previous report, the supposed growth mechanism of the PZO films includes two aspects at least. On the one hand, it is generally believed that the nucleus for crystallization is lacking on Pt substrates. Hence, when films deposited on Pt substrates directly, formation and growth of crystal nucleus are inhomogeneous [14]. On the other hand, neck is formed due to grain boundary motion because the total grain boundary surface energy is reduced during crystallization [15]. Moreover, it is also found from Fig. 3 that grain sizes are quite different for both films. Based on these results, it could be concluded that the final electrical properties of the films have to be tailored by their microstructure.

Fig. 4 presents room temperature frequency-dependent dielectric constant and dielectric loss curves of the two PZO films, which were measured in the range of 20–1000 kHz. With increasing frequency, dielectric constant in both cases is slightly decreased, indicating that some polarization such as space charge is not responded at higher frequency. However, dielectric constant of PZO-1 is much higher than that of PZO-2, which should be the result of their different microstructure. It is also found from Fig. 4 that dielectric loss of both AFE films is less than 3%. It should be noted here that the increase in dielectric loss with increasing frequency is caused by the measurement system, including the hypothesis of the influence of the contact resistance between the probe and the electrode. Similar behavior was also reported in other dielectric thin films [18,19].

Room temperature field-induced polarization hysteresis (P–E) loops of the PZO films are plotted in Fig. 5. Both films show a double hysteresis loop, and no remnant polarization is exited after the remove of electric field. This indicates that both films are stable AFEs at room temperature. Under the same measurement condition, the maximum polarization value is 45 and 18 $\mu C/cm^2$ for PZO-1 and PZO-2, respectively. Meanwhile, PZO-1 shows a squared P–E loop in contrast to PZO-2. The larger maximum polarization value and the squared loops demonstrate that the PZO AFE films from zirconium isopropoxide are more suitable for application in high-energy-storage capacitors.

Temperature dependence of dielectric constant curves of the two PZO AFE films are displayed in Fig. 6, which were detected on heating process and at 100 kHz. With increasing temperature, dielectric constant of both films firstly gradually increases, and then decreases. A same peak is observed at 231 °C in both films, which corresponds to the phase transition from AFE to paraelectric (PE). This temperature, also called Curie point, is consistent with the reported value of PZO bulk ceramic [20]. The inset in Fig. 6 gives dielectric constant curves with respective to dc electric field (*C*–*V*), which were measured at 100 kHz and at room temperature. The electric field was stepped at 8.5 kV/cm increments with a time lag of 0.5 s through the measurement mode: 0 to E_{max}, then E_{max} to $-E_{max}$, and $-E_{max}$ to 0. Obviously, the curves of both PZO films show a similar double-butterfly behavior with four dielectric peaks, which is corresponded to the field-induced phase transition between AFE and FE. This result also demonstrates the AFE nature of the PZO films. According to the peaks of the curves, the obtained switching field for AFE–FE and the reverse field are about 210 kV/cm and 128 kV/cm for both PZ AFE films, indicating that the microstructure in this work have no obvious effect on their phase transition process. It should be mentioned here that the asymmetry character of the curves is caused by the dissymmetry structure of the electrodes.

Fig. 7 shows dc field-dependent current (*J*–*E*) curves of the PZO AFE films. The measurements were also carried out at room temperature and the change of electric field was followed the same model as *C*–*V* curves. Clearly, *J*–*E* curves of the two films display a different characteristic. For the films prepared from zirconium nitrate, the current increases gradually with increasing dc electric field, then declines with decreasing field. However, for the films prepared from zirconium isopropoxide, *J*–*E* curve shows a quite different behavior and four obvious peaks are detected during the

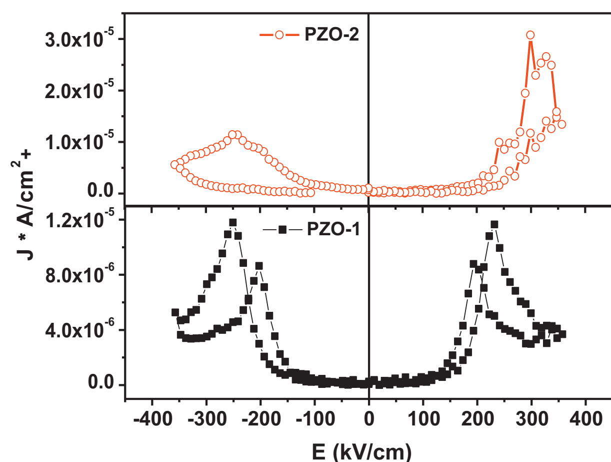

Fig. 7. *J–E* curves of the PZO AFE films from different starting materials.

measurements, which are formed by the phase switching between AFE and FE. It should be pointed out that the obtained current as a function of dc electric field includes leakage current and phase transition current. More detailed explanations on this were reported in our previous work [21]. The difference in *J–E* curves between the two PZO films indicates that sample PZO-1 has a smaller leakage current in contrast to sample PZO-2. As a result, the phase switching current for sample PZO-1 was detected.

4. Conclusions

In conclusion, the starting materials had strong effects on the structure and electrical properties of PZO AFE thin films. As compared with the films prepared from zirconium nitrate, the films from zirconium isopropoxide showed a highly (1 1 1)-preferred orientation and had a more uniform microstructure. As a result, the corresponding PZO films displayed larger dielectric constant and heighten polarization of 45 $\mu C/cm^2$. Moreover, this film also had smaller leakage current and a phase switching current was detected in it. Therefore, in order to obtain AFE films with better dielectric properties, selecting an appropriate raw material is important.

Acknowledgements

The authors would like to acknowledge the financial support from the Research Fund for Higher Education of Inner Mongolia under grant no. NJ09080, the National Natural Science Foundation of China under grant no. 51002071, the Key Project of Chinese Ministry of Education under grant no. 210038, the Chunhui Plan of Chinese Ministry of Education under grant no. Z2009-1-01036, the project of State Key Laboratory of Advanced Technology for Materials Synthesis and Processing (Wuhan University of Technology) under grant no. 2010-KF-5, and the Opening Project of Xinjiang Key Laboratory of Electronic Information Materials and Devices under grant no. XJYS0901-2011-01.

References

[1] F. Jona, G. Shirane, F. Mazzi, R. Pepinsky, Phys. Rev. 105 (1957) 849.
[2] J. Zhai, H. Chen, Appl. Phys. Lett. 82 (2003) 2673.
[3] B. Xu, L.E. Cross, D. Ravichandran, J. Am. Ceram. Soc. 82 (1999) 306.
[4] L.B. Kong, J. Ma, W. Zhu, O.K. Tan, J. Alloys Compd. 322 (2001) 209.
[5] J. Parui, S.B. Krupanidhi, Appl. Phys. Lett. 92 (2008) 192901.
[6] N. Vittayakorn, B. Boonchom, J. Alloys Compd. 509 (2011) 2303.
[7] P. Charoonsuk, S. Wirunchit, R. Muanghlua, S. Niemcharoen, B. Boonchom, N. Vittayakorn, J. Alloys Compd. 506 (2010) 313.
[8] E.M. Alkoy, S. Alkoy, T. Shiosaki, Jpn. J. Appl. Phys. 44 (2005) 6654.
[9] Z. Xu, X. Dai, D. Viehland, Appl. Phys. Lett. 65 (1994) 3287.
[10] L. Wu, D. Xiao, F. Zhou, Y. Teng, Y. Li, J. Alloys Compd. 509 (2011) 466.
[11] H. Chen, C. Yang, J. Zhang, Y. Pei, Z. Zhao, J. Alloys Compd. 486 (2009) 615.
[12] A.S. Mischenko, Q. Zhang, J.F. Scott, R.W. Whatmore, N.D. Mathur, Science 311 (2006) 1270.
[13] B. Xu, Y. Ye, L.E. Cross, J. Appl. Phys. 87 (2005) 2507.
[14] X. Hao, J. Zhai, F. Shang, J. Zhou, S. An, J. Appl. Phys. 107 (2010) 116101.
[15] X. Hao, J. Zhai, X. Yao, J. Am. Ceram. Soc. 92 (2009) 1133.
[16] X. Hao, J. Zhai, Z. Yue, J. Zhou, J. Yang, S. An, J. Cryst. Growth 314 (2011) 151.
[17] L.S. Cavalcante, J.C. Sczancoski, F.S. De Vicente, M.T. Frabbro, M. Siu Li, J.A. Varela, E. Longo, J. Sol–Gel Technol. 49 (2009) 35.
[18] J. Zhai, X. Li, H. Chen, Thin Solid Films 466 (2004) 200.
[19] F.M. Pontes, D.S.L. Pontes, E.R. Liete, E. Longo, E.M.S. Santos, S. Mergulhao, A. Chiquito, P.S. Pizani, F. Lanciotti Jr., J.A. Varela, J. Appl. Phys. 91 (2002) 6650.
[20] X. Dai, J.-F. Li, D. Viehland, Phys. Prev. B 51 (1995) 2651.
[21] X. Hao, J. Zhai, J. Zhou, Z. Yue, J. Yang, W. Zhao, S. An, J. Alloys Compd. 509 (2011) 271.